Impact of structural distortions on the performance of hollow-core photonic bandgap fibers

Eric Numkam Fokoua,* David J. Richardson, and Francesco Poletti

Optoelectronics Research Centre, University of Southampton, Highfield Campus SO17 1BJ, Southampton, UK
**ernf1g10@orc.soton.ac.uk*

Abstract: We present a generic model for studying numerically the performance of hollow-core photonic bandgap fibers (HC-PBGFs) with arbitrary cross-sectional distortions. Fully vectorial finite element simulations reveal that distortions beyond the second ring of air holes have an impact on the leakage loss and bandwidth of the fiber, but do not significantly alter its surface scattering loss which remains the dominant contribution to the overall fiber loss (providing that a sufficient number of rings of air holes (≥5) are used). We have found that while most types of distortions in the first two rings are generally detrimental, enlarging the core defect while keeping equidistant and on a circular boundary the glass nodes surrounding the core may produce losses half those compared to "idealized" fiber designs and with no penalty in terms of the transmission bandwidth.

OCIS codes: (060.4005) Microstructured fibers; (060.2280) Fiber design and fabrication.

References and links

1. F. Poletti, N. V. Wheeler, M. N. Petrovich, N. Baddela, E. Numkam Fokoua, J. R. Hayes, D. R. Gray, Z. Li, R. Slavík, and D. J. Richardson, "Towards high-capacity fibre-optic communications at the speed of light in vacuum," Nat. Photonics **7**(4), 279–284 (2013).
2. Y. Jung, V. A. J. M. Sleiffer, N. Baddela, M. N. Petrovich, J. R. Hayes, N. V. Wheeler, D. R. Gray, E. Numkam Fokoua, J. P. Wooler, H. H.-L. Wong, F. Parmigiani, S.-U. Alam, J. Surof, M. Kuschnerov, V. Veljanovski, H. de Waardt, F. Poletti, and D. J. Richardson, "First demonstration of a broadband 37-cell hollow core photonic bandgap fiber and its application to high capacity mode division multiplexing," in *Proceedings of the Optical Fiber Communications Conference* (2013), paper PDP5A.3 (Postdeadline).
3. P. J. Roberts, F. Couny, H. Sabert, B. J. Mangan, D. P. Williams, L. Farr, M. W. Mason, A. Tomlinson, T. A. Birks, J. C. Knight, and P. St. J. Russell, "Ultimate low loss of hollow-core photonic crystal fibres," Opt. Express **13**(1), 236–244 (2005).
4. E. N. Fokoua, F. Poletti, and D. J. Richardson, "Analysis of light scattering from surface roughness in hollow-core photonic bandgap fibers," Opt. Express **20**(19), 20980–20991 (2012).
5. B. J. Mangan, L. Farr, A. Langford, P. J. Roberts, D. P. Williams, F. Couny, M. Lawman, M. Mason, S. Coupland, R. Flea, H. Sabert, T. A. Birks, J. C. Knight, and P. St. J. Russell, "Low loss (1.7 dB/km) hollow core photonic bandgap fiber," in *Proceedings of Optical Fiber Communication Conference* (2004), paper PDP24.
6. R. Amezcua-Correa, N. G. Broderick, M. N. Petrovich, F. Poletti, and D. J. Richardson, "Optimizing the usable bandwidth and loss through core design in realistic hollow-core photonic bandgap fibers," Opt. Express **14**(17), 7974–7985 (2006).
7. R. Amezcua-Correa, N. G. R. Broderick, M. N. Petrovich, F. Poletti, and D. J. Richardson, "Design of 7 and 19 cells core air-guiding photonic crystal fibers for low-loss, wide bandwidth and dispersion controlled operation," Opt. Express **15**(26), 17577–17586 (2007).
8. R. Amezcua-Correa, F. Gèrôme, S. G. Leon-Saval, N. G. R. Broderick, T. A. Birks, and J. C. Knight, "Control of surface modes in low loss hollow-core photonic bandgap fibers," Opt. Express **16**(2), 1142–1149 (2008).
9. M. H. Frosz, J. Nold, T. Weiss, A. Stefani, F. Babic, S. Rammler, and P. St. J. Russell, "Five-ring hollow-core photonic crystal fiber with 1.8 dB/km loss," Opt. Lett. **38**(13), 2215–2217 (2013).
10. K. Saitoh and M. Koshiba, "Leakage loss and group velocity dispersion in air-core photonic bandgap fibers," Opt. Express **11**(23), 3100–3109 (2003).
11. M.-J. Li, J. A. West, and K. W. Koch, "Modeling effects of structural distortions on air-core photonic bandgap fibers," J. Lightwave Technol. **25**(9), 2463–2468 (2007).

#202083 - $15.00 USD Received 27 Nov 2013; revised 13 Jan 2014; accepted 14 Jan 2014; published 30 Jan 2014

12. F. Poletti, M. N. Petrovich, R. Amezcua-Correa, N. G. Broderick, T. M. Monro, and D. J. Richardson, " Advances and limitations in the modeling of fabricated photonic bandgap fibers," in *Optical Fiber Communication Conference and Exposition and The National Fiber Optic Engineers Conference*, Technical Digest (CD) (Optical Society of America, 2006), paper OFC2.
13. K. Z. Aghaie, M. J. F. Digonnet, and S. Fan, "Experimental assessment of the accuracy of an advanced photonic-bandgap-fiber model," J. Lightwave Technol. **31**(7), 1015–1022 (2013).
14. F. Poletti, "Hollow core fiber with an octave spanning bandgap," Opt. Lett. **35**(17), 2837–2839 (2010).
15. T. Morioka, Y. Awaji, R. Ryf, P. Winzer, D. J. Richardson, and F. Poletti, "Enhancing optical communications with brand new fibers," IEEE Commun. Mag. **50**(2), s31–s42 (2012).
16. T. Murao, K. Saitoh, and M. Koshiba, "Structural optimization of air-guiding photonic bandgap fibers for realizing ultimate low loss waveguides," J. Lightwave Technol. **26**(12), 1602–1612 (2008).
17. F. Poletti and E. Numkam Fokoua, "Understanding the physical origin of surface modes and practical rules for their suppression," in *Proceedings of ECOC 2013*, London (2013), paper Tu.3A.

1. Introduction

Due to rapid recent progress in hollow-core photonic bandgap fiber (HC-PBGF) technology and the highly desirable features of low-latency, ultralow nonlinearity and potential for ultra-low transmission loss that such fibers offer, HC-PBGFs are emerging as an increasingly attractive and credible alternative to all-solid optical fibers in various data transmission applications [1,2]. However, the attenuation levels, which are fundamentally limited in HC-PBGFs by scattering from surface roughness, are yet to be reduced down to the theoretically predicted levels [3,4], restricting the primary current interest to relatively short-haul communication systems. Over the years, numerous efforts in loss reduction have aimed at optimizing the fiber design to reduce the overlap of the guided mode field with the scattering surfaces. Of particular note is the introduction of an antiresonant core surround by Mangan *et al.* which led to the lowest properly documented loss value of 1.7dB/km at 1.56μm reported in 2005 [5] (although a value of 1.2dB/km at 1.625μm was mentioned in [3]). However, the resulting "thick" core surround used supported a multitude of surface modes within the photonic bandgap, which effectively limited the usable bandwidth to only 20nm.

It was later predicted and demonstrated for fibers with a 7-cell core defect, that making the core wall half as thin as the struts in the cladding would help eliminate surface modes, thereby increasing the operational bandwidth [6–8]. In an attempt to expand the usable bandwidth and further reduce the loss for fibers with larger core defects, a number of recently reported HC-PBGFs have been produced without a core tube. This fabrication procedure has however resulted in prominent structural distortions, notably more enlarged core defects, over-expanded air holes on the 6 corners around the core and compressed claddings with different periodicity along the main symmetry axes [1,2,9]. This is believed to be due to imperfectly balanced pressure differences applied to the core and cladding during fabrication. The fact that these fibers still present low loss values prompts the question as to the impact of structural distortions on the optical performance of HC-PBGFs.

Significant theoretical work has been already devoted to understanding and predicting the attenuation one could obtain from a given HC-PBGF design. These studies have typically either neglected the scattering loss contribution and hence considerably underestimated the total loss, or explored ideal structures with perfectly periodic lattices that are visibly different from fabricated ones [10]. Another strand of activity has focused on modeling fiber geometries obtained from scanning electron micrographs of fabricated fibers; however, instrument resolution imposes a constraint on the accuracy of such studies [11,12]. For a full fiber cross-section, the width of a single glass strut is only a few pixels wide, making it difficult for edge-detection routines to determine accurately the boundaries of the cladding air holes. This can be somewhat overcome by focusing on a smaller fiber section containing the core and a reduced number of rings of air holes. Good quantitative agreement between measured and simulated modal properties such as dispersion and mode-field diameter of commercial HC-PBGF has been obtained using this approach, although any reasonable comparison of loss values is foregone by the omission of part of the cladding [13]. On the

#202083 - $15.00 USD Received 27 Nov 2013; revised 13 Jan 2014; accepted 14 Jan 2014; published 30 Jan 2014

other hand, focusing on specific, fabricated fiber samples precludes more systematic studies of particular classes of distortions and identification of structures allowing improved performances.

In this work, we present a simple but generic description of realistic fiber cross-sections and study the impact of a range of structural distortions on the loss and bandwidth properties. We show that the fundamental mode loss is largely unaffected by cladding distortions beyond the second ring of holes around the core and confirm that an exact periodicity in the cladding is not a strict requirement for air-guidance. Our detailed studies reveal that fibers with enlarged corner holes force the core-guided mode field to overlap more prominently with the glass surfaces and therefore to suffer from higher scattering losses. Interestingly, we find that this problem also occurs in fiber designs usually considered to be "ideal", where the pentagonal holes near the core have a much longer side than the hexagonal ones. To solve this problem, we propose an improved fiber design in which the nodes on the core surround are kept equidistant in order to minimize the modal overlap with the scattering surfaces. This new fiber design is also shown to be less susceptible to surface mode induced bandwidth degradation when the core wall thickness is increased allowing a core tube to be incorporated during fabrication. This offers practical benefits in terms of retention of the target structure along the fiber length (and hence increased fiber yield).

2. Definition of the distorted geometry

Figures 1(a) and 1(c) show, respectively, a scanning electron microscope (SEM) image of the cross-section of the fiber we recently reported in [1] and the corresponding idealized representation of the same fiber (with a perfectly regular cladding) built as per the description of references [6,7], using average geometric parameters (Λ, d/Λ, D_c/d) estimated from the SEM image. In this idealized representation, the core defect made by removing 19 unit cells resembles a dodecagon with a nominal diameter of 22μm, 5 times the average cladding pitch ($4.4\mu m$). However, as a result of distortions in the fiber cross section, the measured core diameter is 26μm or 18.2% larger. Figure 1(b) shows the more accurate structure we designed with the method discussed below, and Fig. 1(d) reports the parameters used to generate such a cross-section.

The distortions present in the geometry are easily implemented if rather than focusing on individual air holes and their shape, the cladding is instead regarded as a collection of individual glass nodes interconnected by a web of thin struts. These glass nodes can be moved from their ideal positions to generate any desired cladding distortion and later reconnected to form the transformed air holes [9]. With such an approach, a selected air hole may be enlarged, collapsed, rotated or have any of its corner points undergo a different transformation. Obviously, distorting one hole simultaneously affects some or all of its neighboring holes as well. A number of structural parameters are necessary to build the geometry of Fig. 1(b) so that it resembles that of fabricated structures. First, the fiber core radius (R_c), the number of rings of air holes around the core (N) and the mean radius of the microstructured cladding (*Rcladding*) need to be specified. Secondly, we set the dimensions of the enlarged hexagonal corner holes (L_1,L_2,h_1,h_2), along with those of the air holes on the diagonal (W,H), see Fig. 1 for their description. A tapering of the size of these air holes may be also incorporated if desired. The remaining nodes are then placed so that the cladding resembles that of fabricated fibers by focusing on one $\pi/3$ sector, thereby imposing a C_{6v} symmetry to the generated structure. The parameters crucial to the spectral position of the photonic bandgap are the strut thickness t, the fillet radius r_c and the average spacing between the glass nodes [14]. Imposing that for mass conservation t becomes inversely proportional to the strut length, especially on the core boundary, is essential to ensure accurate results and can have profound impacts on the properties of the fiber.

#202083 - $15.00 USD Received 27 Nov 2013; revised 13 Jan 2014; accepted 14 Jan 2014; published 30 Jan 2014

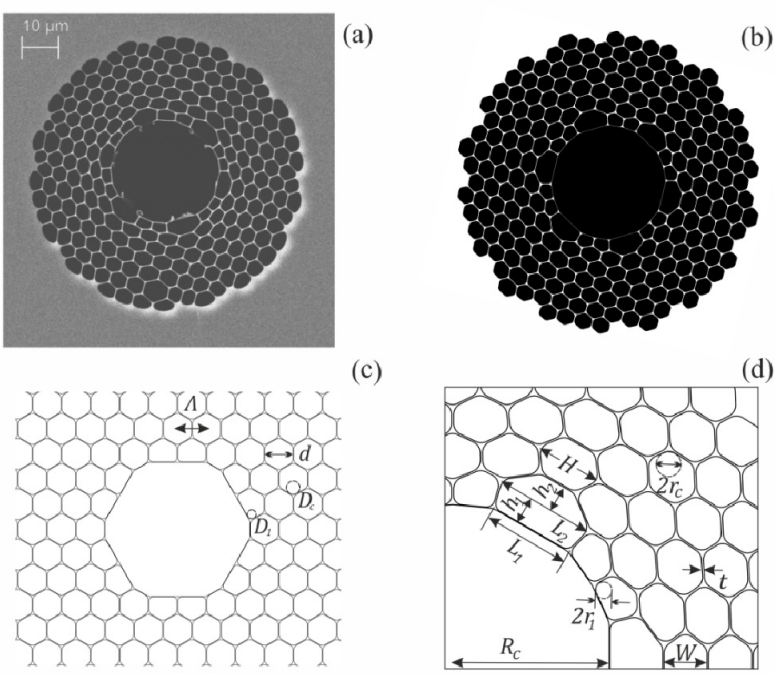

Fig. 1. Geometry description of a HC-PBGF: (a) SEM image of the fiber reported in [1] (b) ideal representation generated with average parameters extracted from the SEM image (c) more realistic distorted profile and (d) parameters required to build distorted fiber geometry.

To illustrate how the distorted geometry allows a much more faithful reproduction of the fiber's optical properties, we compare the calculated differential group delay (DGD) for a few representative mode groups guided in the fiber shown in Fig. 1(c) to measurements performed on the fabricated fiber shown in Fig. 1(a). The results for the 1.55μm wavelength are shown in Fig. 2.

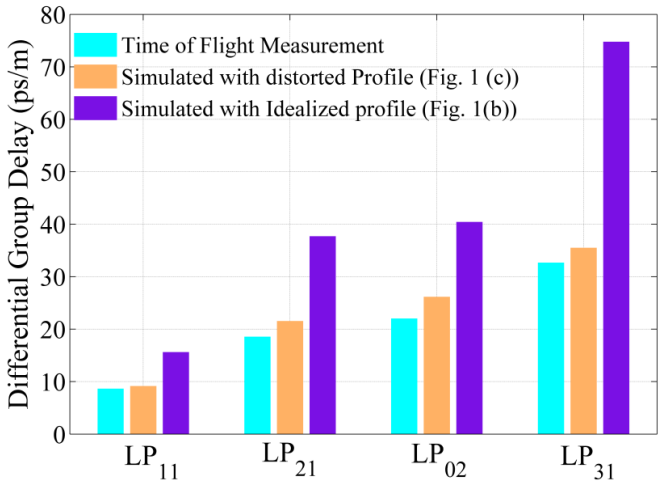

Fig. 2. Measured and simulated differential group delay (DGD) for a few higher order modes at 1.55μm . The DGD was measured using a time-of-flight measurement technique on a 260m long fiber sample. The data shown is the average of measured and simulated values for the individual modes of each mode group. Note that the good agreement between simulation data with a distorted profile and the measurement.

#202083 - $15.00 USD Received 27 Nov 2013; revised 13 Jan 2014; accepted 14 Jan 2014; published 30 Jan 2014

For the comparative analysis presented in the following sections, the simulated fiber loss takes into account contributions from both leakage or confinement, and scattering from surface roughness. The latter is known to impose a fundamental limit on the achievable attenuation in HC-PBGFs, and as recently shown, is the major loss contribution in fibers with ~*dB/km* loss levels with 6 or more rings of air holes outside the core defect [3,4]. To save computation time but without loss of generality, the scattering loss is computed here not by the rigorous treatment formulated in [4], but through the simplified method of calculating the normalized interface field intensity on the fiber's air-glass interfaces [3]:

$$F = \left(\frac{\varepsilon_0}{\mu_0}\right)^{\frac{1}{2}} \frac{\oint_{hole-perimeters} |E|^2 \, ds}{\iint_{cross-section} E \times H^* dA} \tag{1}$$

where ***E*** and ***H*** are the electric and magnetic field vectors of the guided core mode. In this work the scattering loss is calibrated from previous simulations and measurements so that a loss value of 3.5*dB/km* around a wavelength of 1.5μm corresponds to $F = 0.0116\mu m^{-1}$.

3. Impact of cladding size

The microstructure surrounding the core defect determines the spectral position and width of the photonic bandgap. Our study on the impact of distortions begins with an investigation into the effects of non-uniformities far away from the core defect. It is well established that the position and width of the photonic bandgap are determined by the average node size, the average distance separating them and the strut thickness [14]. For a fixed core diameter R_c, increasing the ratio $R_c/R_{cladding}$ by compressing the microstructured cladding leads to a proportional decrease in the average distance between the cladding nodes, ultimately resulting in the photonic bandgap shifting to shorter wavelengths [14]. By altering the cladding size only beyond the second ring outside the core, some insight can be gained into the effect of distortions in this region on the propagation loss of the fiber.

Figure 3 shows plots of loss vs. wavelength for three fibers in which the core and the first two rings of holes are kept the same, while the remainder of the cladding is progressively radially compressed. Fiber A drawn in blue has a core radius $R_c = 13\mu m$, a ratio between core and microstructured cladding diameter of 31% (29% in ideal fibers) and an average strut thickness of *110nm*, which together with the fillet radius $r_c/W = 0.21$ (W being the width of an air hole on the diagonal, see Fig. 1(d)) yield a photonic bandgap centered around 1.7μm . The outer four rings are then modified so that the cladding diameter is 95% smaller for Fiber B shown in green and 90% smaller for Fiber C shown in red. It can be observed that confinement loss, plotted in dotted lines, increases by more than an order of magnitude for each progressive cladding compression, and contributes to a net reduction in the overall transmission bandwidth. The narrower bandwidth results from the more closely spaced nodes (narrowing the photonic bandgap) and a thinner holey air region surrounding the core (increasing the confinement loss). However, at wavelengths well within the bandgap, the three fibers have essentially the same value of total loss, confirming that loss is dominated by scattering from surface roughness, which is mostly unaffected by the structure beyond the second ring.

A first conclusion is therefore that real HC-PBGFs are robust to slight distortions beyond the second ring of air holes, and as a result loss reduction efforts should focus on optimizing the first two rings while ensuring that the outer structure is uniform enough to keep leakage loss at negligible values.

#202083 - $15.00 USD Received 27 Nov 2013; revised 13 Jan 2014; accepted 14 Jan 2014; published 30 Jan 2014

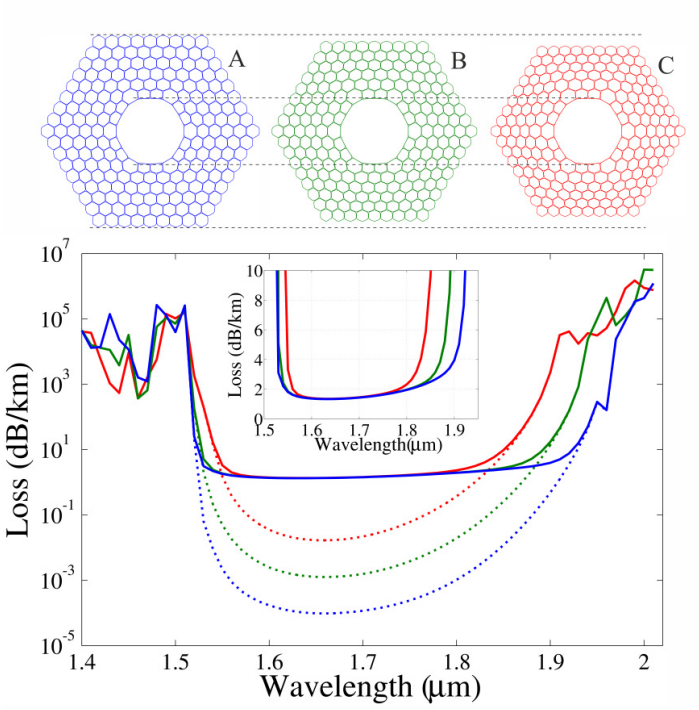

Fig. 3. Impact of cladding size on HC-PBGF loss. Fiber A in blue is close to an idealized and undistorted fiber; in Fiber B and C the cladding beyond the second ring is scaled down to 95% and 90% of its original size, respectively. The dotted lines indicate leakage loss only while the solid lines show the total loss (i.e. leakage + scattering). The inset plots the total loss of the fibers on a linear scale between 0 and 10dB/km.

4. Impact of corner hole size under mass conservation

Besides a radial over-compression of the cladding due to an enlarged core, another frequent distortion present in fabricated HC-PBGFs such as those in [1,2,9] is the presence of six oversized corner holes around the core defect (see Fig. 1(a)). These arise as a natural consequence of surface tension trying to create a circular core surround from an original hexagonal structure. To investigate the impact of such distortions, we have simulated fiber geometries with parameters obtained from the SEM image of Fig. 1(a). The measured core diameter was $2R_c$ = 26μm and the core to cladding diameter ratio was 0.36 with six rings of air holes. This is equivalent to an average spacing of 2.54μm between the glass nodes. The *average* thickness of the cladding struts was estimated to be t = 110nm in the cladding and $t/2$ on average on the core surround ring to account for the absence of a core tube in the fabrication of the fiber. In addition we imposed conservation of the glass volume in the struts, resulting in struts longer than on average being thinner than t and vice-versa. The fillet radius used to round the holes' corners was set to r_c/W = 0.21. In an idealized fiber with core radius R_c, the distance between two nodes everywhere in the cladding would be $l = 2R_c / 5\sqrt{3}$. We changed the corner holes side length L_1 in 6 incremental steps from 1.4l where the nodes on the core wall are nearly equidistant, to 2.4l which is the structure that best resembles the fabricated fiber and is shown in Fig. 1(c). We then computed the mode profiles and loss for all wavelengths across the bandgap for the six resulting fibers and show the results in Fig. 4 below. Also superposed on the figure are the loss plot for the ideal fiber (Fig. 1(b)) and the cutback measurement for the fabricated fiber from [1].

#202083 - $15.00 USD Received 27 Nov 2013; revised 13 Jan 2014; accepted 14 Jan 2014; published 30 Jan 2014

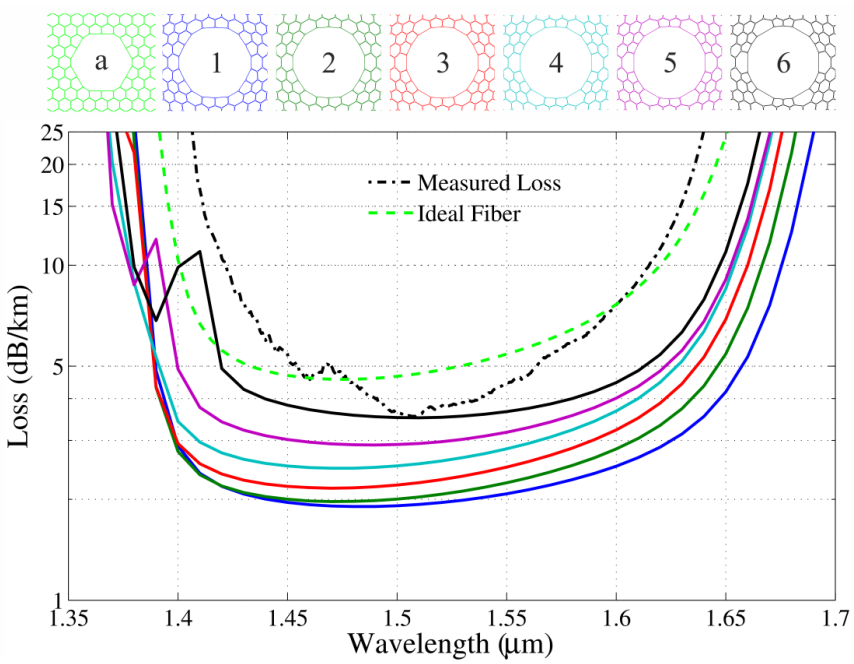

Fig. 4. Impact of corner hole size on the loss of HC-PBGFs. Fibers 1 to 6 have incrementally larger corner holes. The dotted green line shows the loss computed for the idealized fiber shown as (a) while the dash-dot black line is the cutback measurement on the fabricated fiber.

In these fibers, the scattering loss contribution remains dominant when six rings of air holes surround the core. Although the leakage loss contribution in the fiber with the most enlarged corner holes (Fiber 6) is twice as much as for the fiber with the least enlarged ones (Fiber 1), it still only amounts to $0.035 dB/km$ - a small fraction of the total loss. From the plots of Fig. 4, it can be appreciated that fibers with larger corner holes suffer from higher losses. The larger corner holes impose larger gaps between the glass nodes on the core boundary, and such gaps prompt the electric field to overlap more strongly with the scattering surfaces, generating a significantly higher scattering loss. As an illustration of this effect, the time average power flow in the fiber axis direction for the fundamental mode is shown in Fig. 5 for Fiber 1 and 6 having the least and most enlarged corner holes, respectively.

It is striking to point out that the idealized and distortion free structure most routinely used in simulations and usually considered to be the optimized fiber design, see Fig. 1(c), is the one providing the highest loss despite having a core surround designed to preserve the periodicity of the cladding.

This is due to two main reasons. First, the idealized fiber has a core diameter that is 1.18 times smaller than Fibers 1-6. In idealized structures, if the core is enlarged while preserving the cladding periodicity, for example by removing 7, 19, 37… unit cells, the loss is well known to decrease as $\sim R_c^{-3}$ [15]. In the case of our 'distorted' fibers the core is enlarged by compressing the cladding. If we still apply the $\sim R_c^{-3}$ rule (which may be less valid in this case but can still provide an upper limit), the idealized fiber loss is expected to be higher by a factor of $1.18^3 = 1.64$ at most, with respect to that of Fiber 1. However, the actual loss of the idealized fiber is 2.4 times higher than that of Fiber 1, indicating that the equal spacing of the nodes on the core boundary (in Fiber 1) has a significant impact on the fiber loss. As shown by the contour plots of Fig. 5 and verified in numerous simulations we performed, equal spacing of the glass nodes on the core boundary appears to be the optimal design not only for

#202083 - $15.00 USD Received 27 Nov 2013; revised 13 Jan 2014; accepted 14 Jan 2014; published 30 Jan 2014

loss reduction but also for its robustness in avoiding the introduction of surface modes within the bandgap when the core wall thickness is slightly increased (more details below).

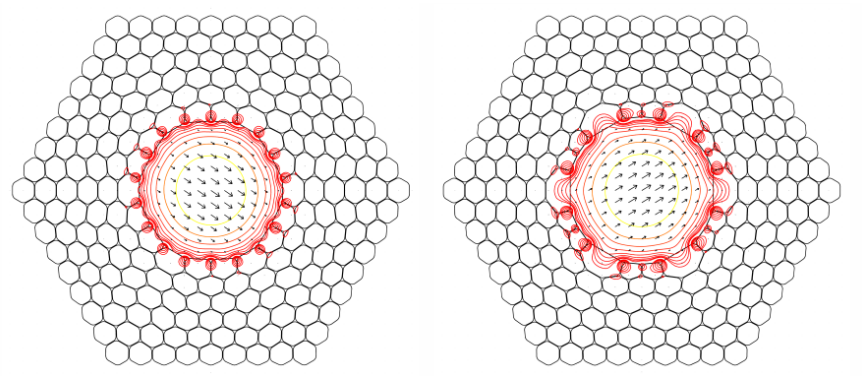

Fig. 5. Contour plots of time average power flow in the z-direction for Fiber 1 (left) and Fiber 6 (right). The contour lines are over a 30dB range and 2dB apart. Note how large gaps on the core boundary prompt the guided mode to overlap more strongly with the air-glass interfaces.

5. Core surround design and surface modes

Previous work on idealized fiber structures has established that a uniformly thick core wall with half the thickness of the struts in the cladding can eliminate surface modes within the photonic bandgap, thereby substantially increasing the usable bandwidth while also keeping the loss at low values [6–8,16]. Whilst very useful, this simple empirical rule does not provide a physical understanding of the origin of surface modes and does not necessarily hold in more distorted structures like those in Fig. 4. We have observed that when distortions result in significantly uneven node spacing on the core boundary (such as in Fibre 6), a uniformly thick core surround with half the thickness of the cladding struts ends up supporting one or more surface modes. Our recent work also points out that when mass conservation is applied to the core wall in such cases, it is the shorter but thicker struts on the core wall that support surface modes [17]. Besides, the nodes on the core surround may themselves support surface modes if their size is not matched to that of the cladding nodes [17]. Here we show that the optimized structure where the core nodes are equidistant is also more robust to surface modes as it tolerates increases in the core thickness without significant loss or bandwidth penalty.

The study of fiber structures with thicker core walls is a useful one since the incorporation of a core tube in the initial stack is known to simplify the structural control during fabrication and to significantly improve both the stability and yield of the draw. We studied two different sets of fibers as a function of core wall thickness, the first set with equally spaced nodes on the core boundary and the second with enlarged corner holes such as Fiber 5 (Fig. 4). Figures 6 and 7 show the calculated loss for these two sets of fibers, along with the effective index plots as a function of increasing core wall thickness.

#202083 - $15.00 USD Received 27 Nov 2013; revised 13 Jan 2014; accepted 14 Jan 2014; published 30 Jan 2014

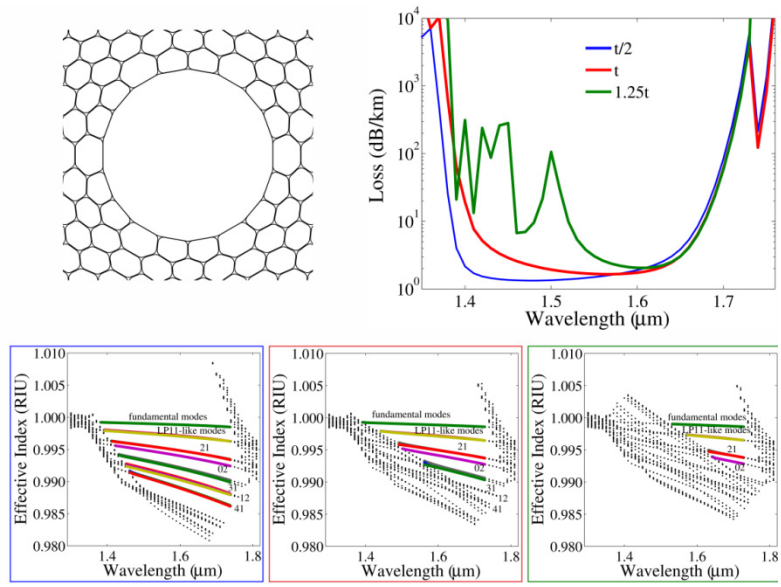

Fig. 6. Impact of core wall thickness on loss and modal content for a HC-PBGF with equal node spacing on the core boundary. The curve labeled *t*/2 is for a fiber with no core tube, whereas those labeled *t* and 1.25*t* are for fibers with core tubes that are as thick and 1.25 times thicker than the capillaries in the starting stack. As the core wall is thickened, surface modes move within the bandgap from the short wavelength edge, indicating they are located in the struts [17].

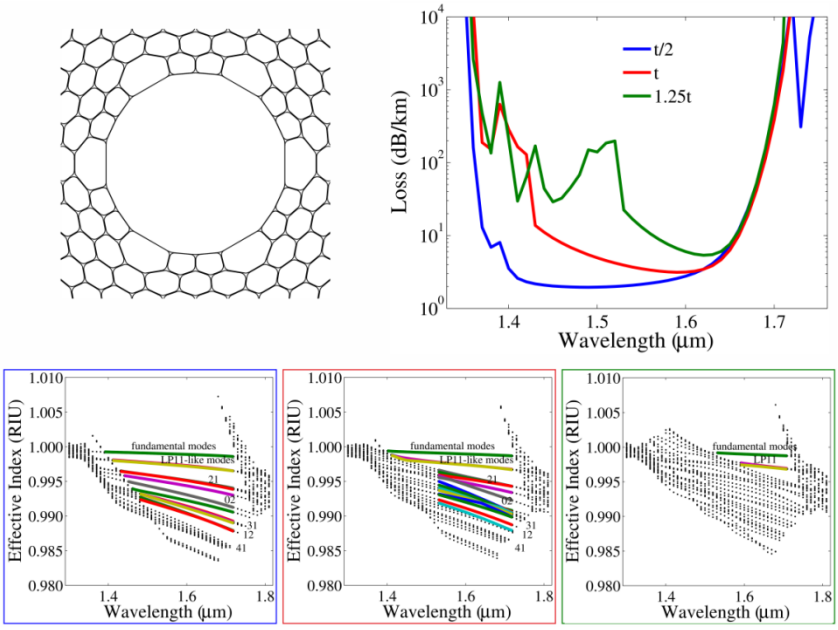

Fig. 7. Impact of core wall thickness on loss and modal content for a HC-PBGF with a six distorted and enlarged corner holes. For this distorted fiber, increasing the core wall thickness results in more severe loss and bandwidth penalties as compared to the fiber shown in Fig. 6.

When mass conservation is applied to the core wall in the absence of a core tube in the preform (*t/2*), the fundamental mode bandwidth is wide for both fibers and the loss remains

#202083 - $15.00 USD Received 27 Nov 2013; revised 13 Jan 2014; accepted 14 Jan 2014; published 30 Jan 2014

low. Additionally, the effective indices of all the guided modes are clearly separated and their properties can be easily studied.

Interestingly, doubling the core wall thickness under mass conservation (by assuming an initial preform with a core tube as thick as the cladding capillaries) does not result in a great bandwidth or loss penalty for fundamental mode transmission in the first fiber. Its minimum loss increases from 2 to $2.4 dB/km$ with only a $10nm$ reduction in the $3dB$ bandwidth. The reduction in bandwidth and increase in loss is clearly more noticeable for the fiber with large corner holes, going from a minimum of $2.9 dB/km$ over a $3dB$ bandwidth of $230nm$ to $4.6 dB/km$ over $160nm$. In both cases, the surface modes introduced cross the fundamental mode near the short wavelength edge of the photonic bandgap, guaranteeing that the bandwidth for the fundamental mode remains largely unaffected. Higher order modes however interact with these surface modes near the center of the bandgap and therefore suffer a severe reduction in bandwidth. This suggests that the design with equal node spacing on the core boundary not only provides the lowest loss but it is also more tolerant to a thicker core wall.

Further increasing the core wall thickness beyond this point can have limiting effects on both fibers' performances. For example, when a core tube 1.25 times thicker than the capillaries is used, surface modes anti-cross with the fundamental mode near the middle of the bandgap, resulting in higher losses and severe reduction in bandwidths. Once again, the penalties are higher for the distorted structure. Also noteworthy is the fact that with thicker core surrounds, the degeneracy for higher order mode groups in the distorted fiber is generally broken and the differential loss with the fundamental mode substantially increased.

6. Conclusion

In summary, we have presented a new generic method for modeling HC-PBGF geometries with arbitrary distortions in their cross section such as core expansion or compression and distortions of selected air holes. This method allows one to model the properties of fabricated fibers that contain moderate cross-sectional distortions. For example, we have shown it can accurately predict the differential group delay between modes, or equally, other fiber properties that depend on exact core shapes, such as effective area or percentage of power in the glass.

Finite element method simulations on HC-PBGFs with distorted profiles have shown that loss in these fibers remains largely dominated by scattering from surface roughness which occurs predominantly in the first two rings of air holes near the core defect. A study on the effect of enlarged corner holes in the core surround, often present in state-of-the-art large core fibers, has revealed how these distorted holes force the field to overlap more strongly with the scattering surfaces causing a higher scattering loss. These observations have led us to propose an improved and optimized low-loss fiber design in which the nodes on the core boundary are equidistant. Such a design is more tolerant to the inclusion of a core tube of appropriate thickness, which would simplify the fabrication of the fibre while avoiding the introduction of surface modes within the photonic bandgap.

Acknowledgments

The authors would like to thank colleagues Natalie Wheeler, Marco Petrovich, Naveen Baddela and John Hayes for fabricating the fiber and collecting its SEM image, for kindly providing cutback measurement data and for useful discussions. This work was supported by the EU 7th Framework Programme under grant agreement 258033 (MODE-GAP) and by the UK EPSRC through grant EP/H02607X/1.